Pile-up Rejection in the High Granularity Time Detector for the High Luminosity LHC

Paul McNulty, George Mason University

19/08/2016

Abstract

The High Granularity Timing Detector, a proposed upgrade to the Liquid Argon Calorimeter during the transition to the High Luminosity LHC, will provide increased resolution in the time domain and offer an avenue for efficiently mitigating the expected increase in pile-up jets. This study analyzes how effectively current algorithms are using a signal jet peak calculation to disentangle desired information from other events. Two samples, one with only hard-scattering events and another that also included pile-up events, were used. A transverse momentum range of 30GeV to 70GeV and pseudo-rapidity range of 2.4 to 4.8 divided the sample to see how the HGTD performed when calculating the signal peak for each jet and how many cells had detections in and out of that peak for each sample.

Introduction

A High Granularity Timing Detector (HGTD) has been proposed to cope with the large increase of pile-up interactions that will result from the upgrade to the High Luminosity LHC, scheduled for 2022-2023. The increase in luminosity will create an increase of pile-up data. This noise produced from uninteresting physics, in this study mostly diffraction interactions between protons as opposed to hard-scattering events, is difficult to disentangle from the desired data. An increase of resolution in the time domain, provided by the HGTD, would allow for better reconstruction of jets by working with the Liquid Argon (LAr) calorimeter to reject pile-up hits. Ensuring that this mechanism is precise is essential for teasing out the details of the decays involved. The purpose of this study is to try to understand how well current algorithms are handling the pile-up rejection. The HGTD would fit in front of the LAr calorimeter end-cap and aid the Electromagnetic Calorimeter End Cap (EMEC) and the LAr Forward Calorimeter (FCal) as shown in **Figure 1**.

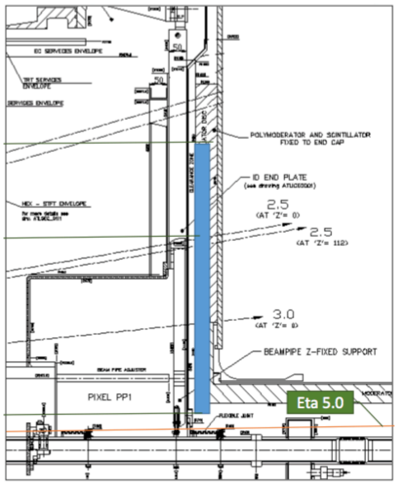

Figure 1: Depiction of where the HGTD will fit within the LAr calorimeter and range of η coverage [3].

The data analyzed here was produced via Monte Carlo simulations using an HGTD configuration with four evenly spaced silicon plates, each of outer radius 600mm and inner radius 50mm. The data samples lack “time-smearing”, which makes all collisions happen at once; have “vertex-smearing”, which accounts for a collision’s ability to happen at any point in the crossing region; and have a 30ps smearing of the hits that is applied to simulate the silicon detectors.

Two data samples that differ in the maximum number of collisions per beam crossing (μ) are used. One was produced without pile-up, that is, only hard-scatter events (μ=0), and the other was produced with high pile-up (μ=200) consistent with the order of magnitude increase in luminosity expected for the HL-LHC [4]. Each contains vector boson fusion (VBF) events, in which quarks produced in hard-scattering collisions decay to W or Z bosons and lighter quarks. The W or Z bosons can interact to create something interesting, such as a Higgs, while the lighter quarks hadronize and create jets in the acceptance of the HGTD.

Analysis

The data samples are stored in the form of ROOT TTrees, which are data structures that contain a number of variables and a list of associated values for each variable. The TTrees used here each contain variables corresponding to the reconstructed jet data and to the true jet values, and were generated by Jose Benitez [2]. As the true values are the same for each sample, they are used to generate a new TTree by selecting one truth variable, matching it to a truth variable in the other TTree, and then obtaining all desired reconstructed quantities that corresponded to that entry from each sample. This ensures that each variable value in the new TTree has a counterpart from each sample and that each reconstructed value is truth-matched.

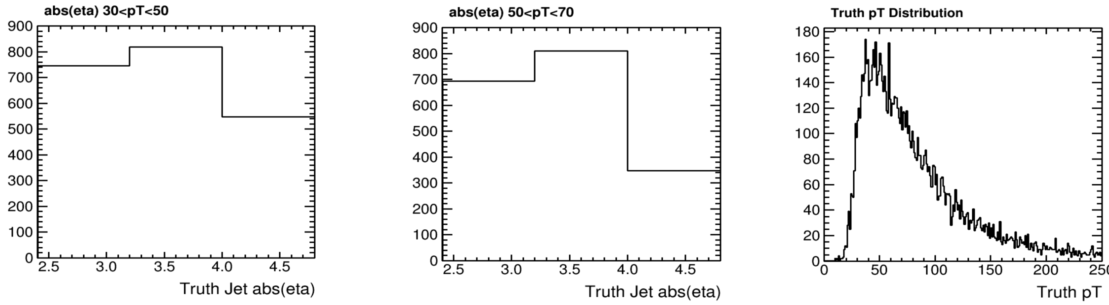

Figure 2: At left and center respectively is shown the distribution of jets as a function of η after selecting 30GeV<p_T<50GeV and 50GeV<p_T<70GeV. At right is shown the truth p_T distribution for the entire sample containing 12159 jets.

In all, the μ=0 sample started with 17179 events and the μ=200 started with 9249. Of these, 12159 jets can be truth-matched between the two samples. The study is further restricted to two transverse momentum regions: 30GeV<p_T<50GeV and 50GeV<p_T<70GeV, and three pseudo-rapidity (η) regions: 2.4<|η|<3.2, 3.2<|η|<4.0, and 4.0<|η|<4.8. These η regions correspond to the EMEC and FCal respectively. The algorithm being analyzed is only applied to jets with p_T<70GeV as most pile-up jets have a p_T value below this. **Figure 2** shows how this divides the jets as well as the total jet sample truth p_T. There are 5490 jets within the 30GeV-70GeV region.

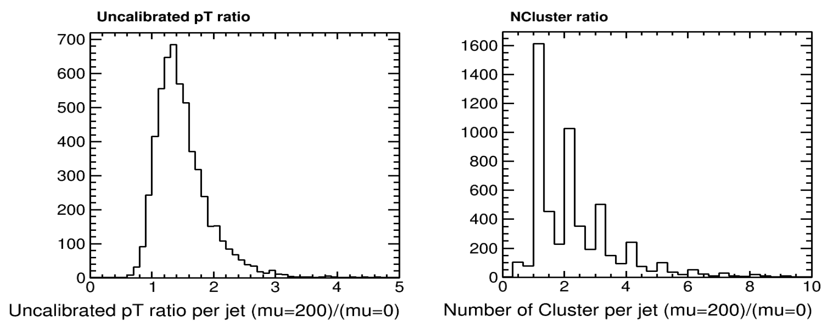

Figure 3: At left is shown the ratio of the uncalibrated reconstructed p_T of the μ=200 sample to the μ=0 sample. At right is the ratio of the number of clusters of the μ=200 to the μ=0 samples in the LAr calorimeter for this p_T region.

Figure 3 depicts the ratio of the uncalibrated reconstructed p_T values of the μ=200 sample to the μ=0 sample for the 30GeV-70GeV region. This shows that for the μ=200 sample generally has a higher transverse momentum for each of its jets. Also given in **Figure 3** is the ratio of the number of clusters for this p_T region of the μ=200 sample to the μ=0 sample, showing a much higher incidence of clusters per jet for the μ=200 sample. The clusters correspond to the LAr calorimeter and are used to define the cells in the HGTD that a signal jet would have passed through.

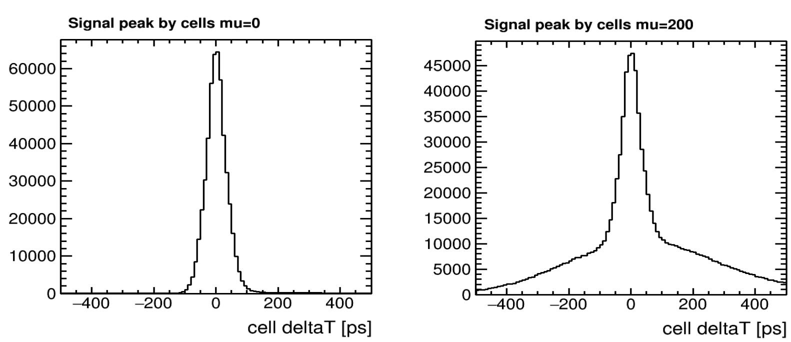

Figure 4: Shown at left and right respectively is the signal peak distribution based on the number of cells hit for the mu=0 and mu=200 samples.

In the data sample generation, there is an algorithm that obtains the peak signal mean by finding the time slice (in picoseconds) that has the highest number of cells triggered for each jet. The signal peak is used to discriminate pile-up jets from signal jets as signal jets have a larger concentration of cells on the signal peak when compared to pile-up jets [1]. **Figure 4** shows that even in the sample with high pile-up, when cells are being hit randomly, a signal jet creates a clear peak above the background. To test how well the peak finding algorithm determines the correct timing cells, the peak position of each μ=200 jet is compared to the peak position of the corresponding μ=0 jet. The number of jets in the μ=200 sample which have a correctly identified signal peak is determined by requiring that the signal peak time matches that of the μ=0 jet within 20ps. This number is then divided by the total number of jets in each of the p_T and η regions to give the fractions of jets that are in the signal peak for each region. These plots and associated fractions can be seen in **Figure 5**, with the fractions also given in **Table 1**.

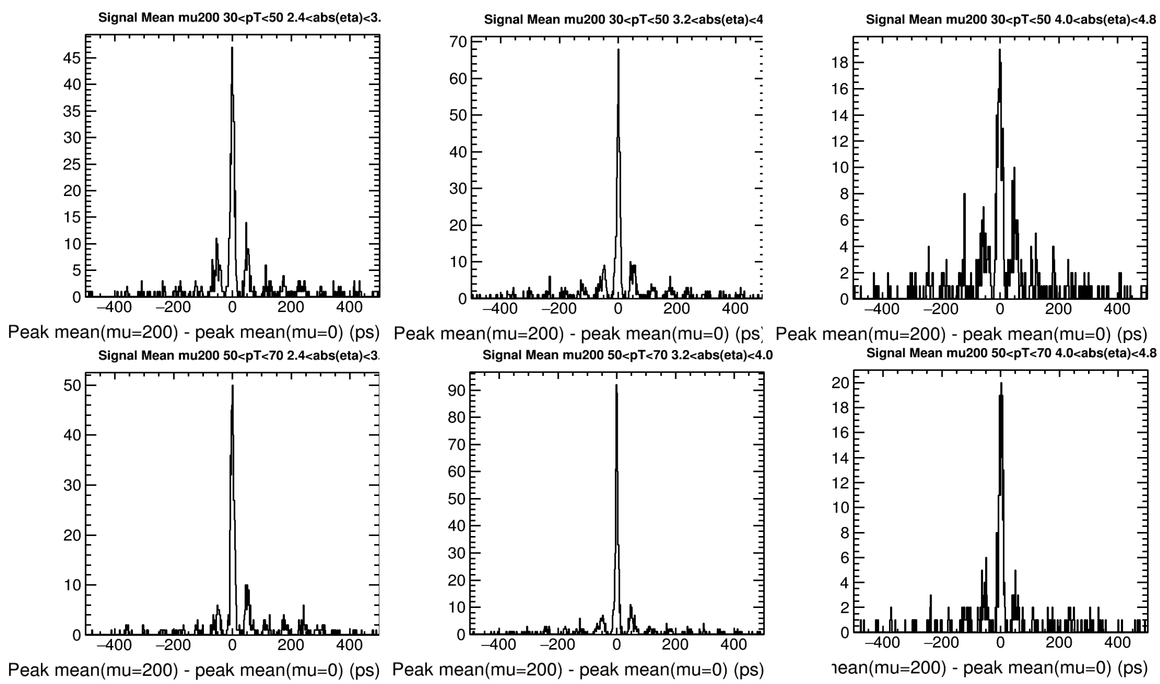

Figure 5: The top row shows the signal mean (dT peak) in the μ=200 sample for each η region and $30GeV<p_T<50GeV$ while the bottom row shows the same for each η region and $50GeV<p_T<70GeV$. The fractions of jets in the peak for the top row (left to right) are: $\mathbf{f_{peak}}$= **0.45**, **0.47**, and **0.34**. For the bottom, the fractions are: $\mathbf{f_{peak}}$= **0.53**, **0.58**, and **0.45**.

Depicted in **Figure 6** is the number of cells triggered in the signal peak. Cells are defined as in-time if they are triggered within 30ps of the signal peak mean. The HGTD rejects out-of-time pile-up, and so pile-up that coincides with the signal mean is still counted to some extent. This is demonstrated more clearly in **Figure 7**, which shows the ratio of the number of cells per jet in the signal peak for the μ=200 to the μ=0 sample. These two figures can be contrasted with **Figures 8** and **9** that show the number of cells triggered outside of the signal peak and the same ratio for those values. **Figures 8** and **9** show just how many more off-signal-peak cells are triggered in the μ=200 sample, which can then effectively be discarded. The mean and RMS values for the graphs in **Figures 7** and **9** are displayed in **Table 2** and **3** respectively.

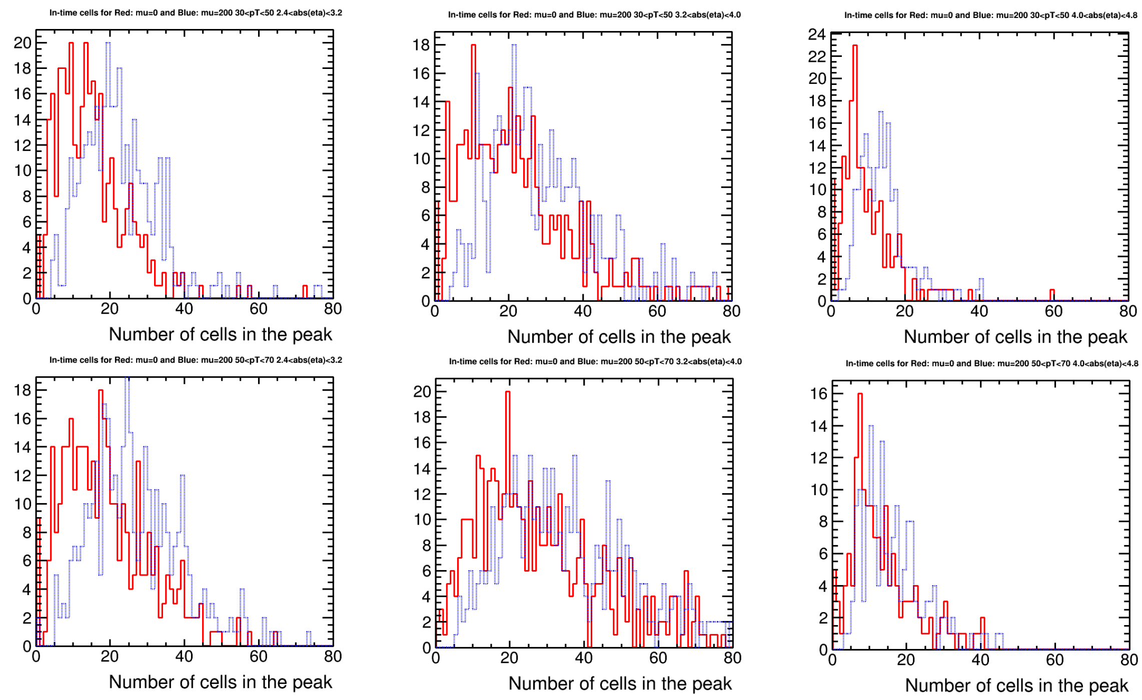

Figure 6: The top row shows the number of cells triggered in the dT peak for each η region and 30GeV<p_T<50GeV while the bottom row shows the same for each η region and 50GeV<p_T<70GeV. The μ=0 sample is shown in the red solid line, while the μ=200 sample is shown in the blue dashed line.

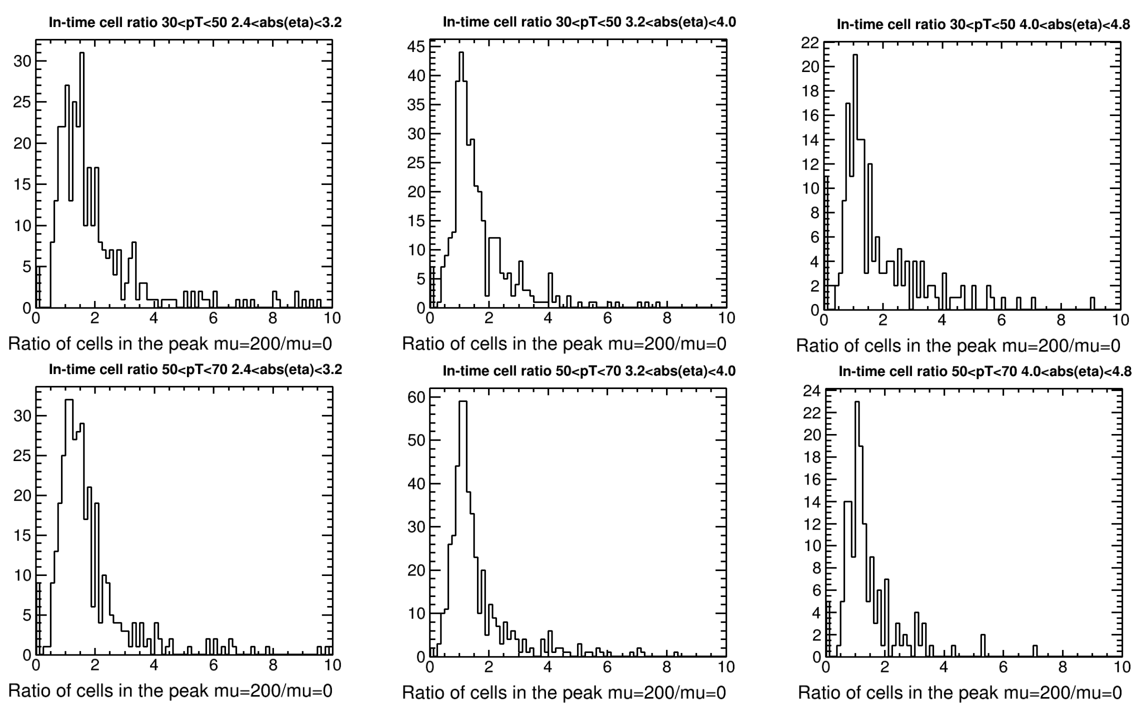

Figure 7: The top row shows the ratio of the number of cells triggered in the dT peak for the μ=200 to the μ=0 sample for each η region and 30GeV<p_T<50GeV while the bottom row shows the same ratio for each η region and 50GeV<p_T<70GeV. These plots correspond only to jets whose peak time is required to match.

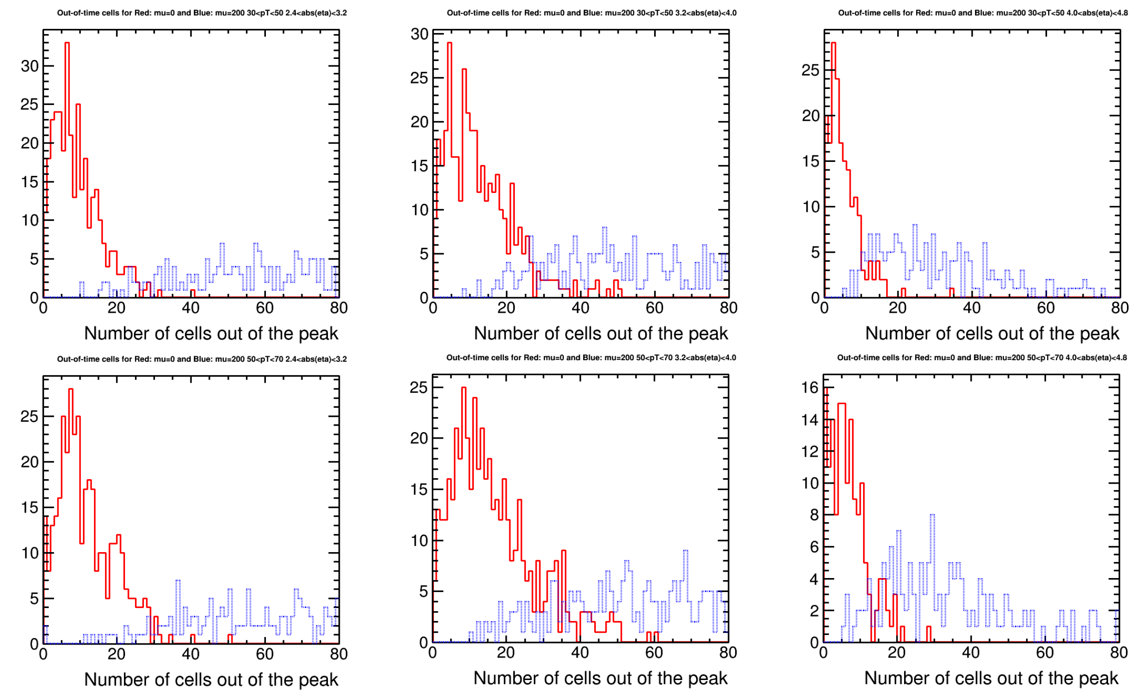

Figure 8: The top row shows the number of off-signal peak cells triggered for each η region and $30\text{GeV}<p_T<50\text{GeV}$ while the bottom row shows the same for each η region and $50\text{GeV}<p_T<70\text{GeV}$. The mu=0 sample is show in the red solid line, while the mu=200 sample is shown in the blue dashed line.

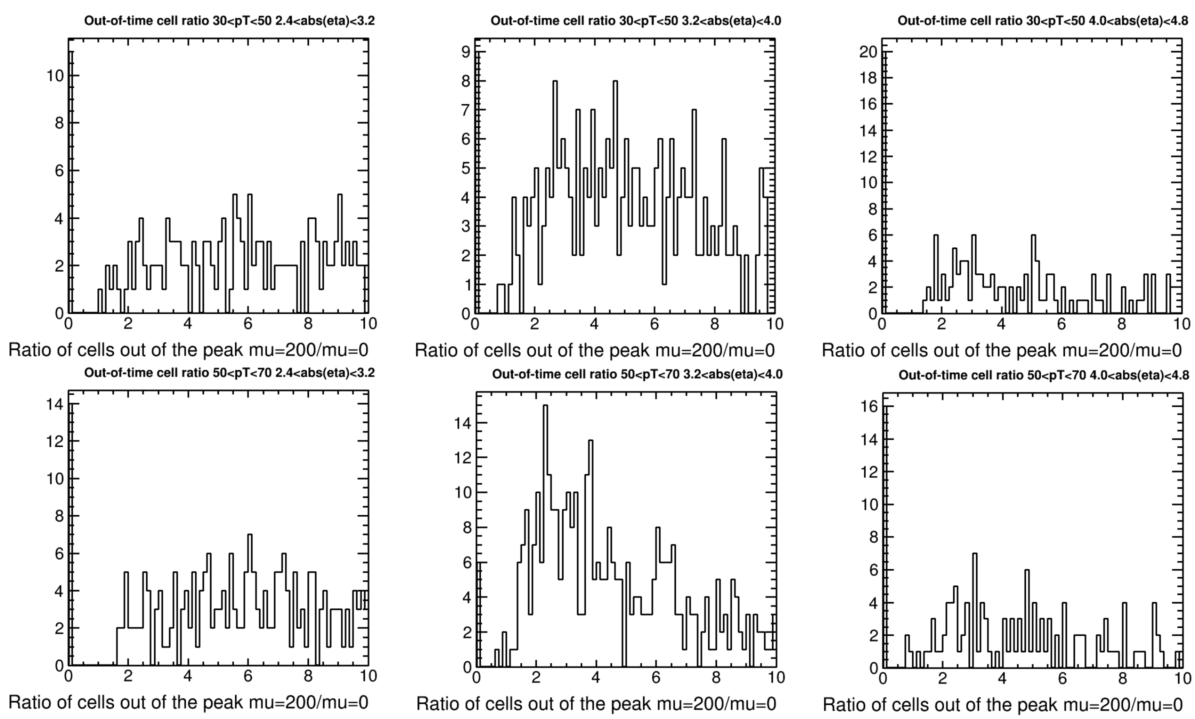

Figure 9: The top row shows the ratio of the number of cells triggered off of the dT peak for the μ=200 to the μ=0 sample for each η region and $30\text{GeV}<p_T<50\text{GeV}$ while the bottom row shows the same ratio for each η region and $50\text{GeV}<p_T<70\text{GeV}$. These plots correspond only to jets whose peak time is required to match.

Results

	2.4<|η|<3.2	3.2<|η|<4.0	4.0<|η|<4.8
30GeV<p_T<50GeV	0.45	0.47	0.34
50GeV<p_T<70GeV	0.53	0.58	0.45

Table 1: Tabulated above are the fractions of jets within the dT signal peak for the μ=200 in each of the p_T and η ranges. These are the same fractions calculated via the histograms in **Figure 5**.

	2.4<|η|<3.2		3.2<|η|<4.0		4.0<|η|<4.8	
	Mean	RMS	Mean	RMS	Mean	RMS
30GeV<p_T<50GeV	2.06	1.76	1.75	1.53	1.79	1.43
50GeV<p_T<70GeV	1.81	1.50	1.71	1.63	1.41	0.97

Table 2: Tabulated above are the mean and RMS values calculated for the in-peak cell ratio of the μ=200 sample to the μ=0 sample. These are for the histograms shown in **Figure 7**.

	2.4<|η|<3.2		3.2<|η|<4.0		4.0<|η|<4.8	
	Mean	RMS	Mean	RMS	Mean	RMS
30GeV<p_T<50GeV	7.15	3.84	6.01	3.44	5.04	3.74
50GeV<p_T<70GeV	6.82	3.61	5.26	3.28	4.63	3.30

Table 3: Tabulated above are the mean and RMS values calculated for the out-of-peak cell ratio of the μ=200 sample to the μ=0 sample. These are for the histograms shown in **Figure 9**.

Conclusion

We have studied the effects of pile-up interactions on hard-scatter signal jets in HL-LHC conditions. Using our current peak finding algorithm, we find that the signal peak is correctly found >45% of the time for jets in the EMEC, and that this percentage degrades as the jets move to the second portion of the FCal. Furthermore, jets of lower p_T also have a lower chance of being placed into the correct peak. The ratios for the in-time cells are not very well defined, as better performance would have led to a narrower peak around one, as opposed to the wide distributions shown in **Figure 7**. As demonstrated in **Figure 8**, **p**ile-up can add two to ten times the number of out of time cells per jet.

Acknowledgments

This work was supported by the International Research Experiences for Students (IRES) grant, number 1358071, from the National Science Foundation. I would like to thank S. Argyropoulos, J. Benitez, U. Mallik, and S. Yang of the University of Iowa for providing scientific insight and guidance during my time here at CERN and P. Rubin of George Mason University for facilitating this experience.

References

1. Benitez, Jose: 03 June, 2016. “Pile-up rejection studies”, HGTD Meeting.
ATLAS internal presentation.

2. Benitez, Jose: August, 2016. Data samples for simulated HGTD jet reconstruction.

3. Mallik, Usha: 09 June, 2016. “Status of the High Granularity Timing Detector (HGTD)”, LAr General Meeting.
ATLAS internal presentation.

4. Rossi, Lucio & Brüning, Oliver: August, 2012. “High Luminosity Large Hadron Collider: A description for the European Strategy Preparatory Group.”
https://cdsweb.cern.ch/record/1471000/files/CERN-ATS-2012-236.pdf